Interactions of CO_2 with various functional molecules

Han Myoung Lee,* Il Seung Youn, Muhammad Saleh, Jung Woo Lee and Kwang S. Kim*

The CO_2 capturing and sequestration are of importance in environmental science. Understanding of the CO_2-interactions with various functional molecules including multi-N-containing superbases and heteroaromatic ring systems is essential for designing novel materials to effectively capture the CO_2 gas. These interactions are investigated using density functional theory (DFT) with dispersion correction and high level wave function theory (resolution-of-identity (RI) spin-component-scaling (scs) Möller–Plesset second-order perturbation theory (MP2) and coupled cluster with single, double and perturbative triple excitations (CCSD(T))). We found intriguing molecular systems of melamine, 1,5,7-triazabicyclo[4.4.0]dec-5-ene (TBD), 7-azaindole and guanidine, which show much stronger CO_2 interactions than the well-known functional systems such as amines. In particular, melamine could be exploited to design novel materials to capture the CO_2 gas, since one CO_2 molecule can be coordinated by four melamine molecules, which gives a binding energy (BE) of $\sim$85 kJ mol^{-1}, much larger than in other cases.

1. Introduction

Carbon dioxide (CO_2) is an important green-house gas, which is known to cause serious environmental damage to global weather and human life.[1–3] Power plant flue gases contain about 75% N_2, 14% CO_2, and 10% moisture. Natural gas reserves contain about 40% CO_2 and N_2 gases.[4] Since CO_2 gas can be converted into diverse valuable organic molecules, it is highly desirable to develop novel materials that capture CO_2 selectively.[5,6] Recently, new intriguing methods have been introduced for CO_2 capture, storage, and utilization.[7,8] Various materials are being developed, such as metal organic frameworks (MOFs),[9–12] zeolite-like sorbents,[13,14] covalent organic frameworks (COFs),[15] polymers with light organic functional groups,[16–19] boron nitride nanotubes,[20] and many kinds of amines including aminoalcohols,[21–23] aqueous ammonia,[24] and ionic liquids.[25,26] However, simple MOF and zeolite materials show low capacity for separating CO_2 from combustion–exhaust gas mixtures.[6] The amine-based wet processes of CO_2 capture show the degradation problem of amines. The CO_2-covalent bonding interactions by amines, ammonia, and ionic liquids consume high energy in regeneration cycles. Furthermore, the aqueous ammonia processes show ammonia loss.[27–30] Various functionalized MOF/zeolite materials have been designed for selective CO_2 capture,[31] and their general functional group is an amine.[32–34] Recently a N-containing polymer sphere was reported to show high CO_2 adsorption capacity.[35] In this material the porous carbon spheres contain intrinsic nitrogen-containing groups. The cooperative CO_2-interactions enhance the CO_2 adsorption enthalpy with the CO_2-interaction energy of a functional group.[19,33] To reduce the degradation problem of amines, aromatic molecules can be used to enhance the stability. Substituted aromatic or heteroaromatic systems can have enhanced CO_2-BEs as compared with benzene.[19,36] On the other hand, CO_2 shows some solubility by physisorption in non-polar or weak polar solvents such as benzene, chloroform and dichloromethane.[37,38] Since CO_2 capture by physisorption shows low CO_2-release energy, many CO_2 capture materials have been developed based on physisorption. It is thus vital to understand the physisorption strengths of CO_2 with many functional groups/molecules. However, limited theoretical investigations were performed.[39–44] Moreover, systematic investigation employing reliable high level *ab initio* methods has hardly been reported for the CO_2 interactions with diverse functional molecules. Therefore, we have systematically selected various functional molecules and calculated their BEs with CO_2, using reliable high-level computational methods. We have found intriguing functional molecules showing large CO_2-interaction energies, which can be used to design novel materials to capture CO_2. Since ionic forms must have counter parts or special conditions to be used to capture CO_2, ionic forms are excluded in this study.

2. Computational details

The CO_2 interactions with various functional molecules were calculated at the M06-2X[45] level with the aug-cc-pVDZ basis set (abbreviated as aVDZ) and the resolution-of-identity (RI)

Center for Superfunctional Materials, Department of Chemistry, Ulsan National Institute of Science and Technology (UNIST), Ulsan 689-798, Korea. E-mail: hmlee@unist.ac.kr, kimks@unist.ac.kr

This journal is © the Owner Societies 2015

Phys. Chem. Chem. Phys., 2015, **17**, 10925–10933 | **10925**

spin-component-scaling (scs) Möller–Plesset second-order perturbation theory (MP2) (RI-scs-MP2)[46,47] level with the aug-cc-pVTZ (aVTZ) basis set. The geometries were fully optimized without symmetry constraints at each calculation level. The M06-2X functional (hybrid-meta GGA with dispersion correction) has shown good performance in the investigation of the dispersion interaction as well as the electrostatic interaction (H-bonding, H–π interaction, π–π interaction, additional electrostatic and induction energies of neutral and charged dimeric systems).[48] Single point (SP) calculations using the RI-coupled cluster theory with single, double and perturbative triple excitations (RI-CCSD(T)) were performed by employing the aVTZ and aug-cc-pVQZ (aVQZ) basis sets at the RI-scs-MP2/aVTZ geometries. The CO_2-BEs were calculated at the complete basis set (CBS) limit at the RI-CCSD(T) level with the aVTZ and aVQZ basis sets by employing the extrapolation approximation.[49,50] The complete basis set (CBS) energies were estimated with the extrapolation scheme utilizing the electron correlation error proportional to N^{-3} for the aug-cc-pVNZ basis set ($N = 3$: T, $N = 4$: Q). It is generally known that the zero-point-energy (ZPE)-uncorrected BE ($-\Delta E_e$) is closer to the experimental CO_2-adsorption enthalpy (ΔH_{ads}) than the ZPE-corrected BE ($-\Delta E_0$).[19,51] Therefore, the values of $-\Delta E_e$ are reported as the CO_2-BEs.

Polar σ-bonding functional molecules give significant electrostatic interactions with CO_2. Aromatic and heteroaromatic functional molecules give significant dispersion force contributions as well as electrostatic interaction contributions. We analyzed the compositions of BEs using symmetry-adapted perturbation theory (SAPT) at the DFT-PBE0 level with the aVDZ basis set, so-called DFT-SAPT.[52] The energy components are the electrostatic energy (E_{es}), the effective induction energy including the induction-induced exchange energy ($E_{ind}{}^\star = E_{ind} + E_{ind\text{-}exch}$), the effective dispersion energy including the dispersion-induced exchange energy ($E_{disp}{}^\star = E_{disp} + E_{disp\text{-}exch}$), and the effective exchange repulsion energy with the induction-induced and dispersion-induced exchange energies excluded ($E_{exch}{}^\star = E_{exch} - (E_{ind\text{-}exch} + E_{disp\text{-}exch})$).[53] In this study, the asymptotically corrected PBE0 (PBE0AC) exchange–correlation (xc) functional with the adiabatic local density approximation (ALDA) xc kernel was used. In the PBE0AC-SAPT calculations, a purely local ALDA xc kernel was used for the hybrid xc functional.

The interaction energies were corrected with the basis set superposition error (BSSE) at the M06-2X and RI-CCSD(T) levels of theory. The RI-scs-MP2 method is known to produce slightly underestimated interaction energies,[47] thus, the BSSE corrections were not carried out at the RI-scs-MP2 level. Thermal energies were calculated by employing the M06-2X harmonic vibrational frequencies. The calculations were performed by using the Turbomole package[54] and the Molpro package.[55]

3. Results and discussion

3.1. Understanding of CO_2 interactions with various normal functional molecules

The M06-2X CO_2-binding structures and energies (in kJ mol^{-1}) of all the functional molecules considered here are given in

Fig. 1 and Table 1. The first five structures show simple electrostatic interactions of each polar molecule with CO_2. Among them, NH_3 having the largest BE ($-\Delta E_e = 14.1$ kJ mol^{-1}) with CO_2 implies that the sp^3 nitrogen atom is the best electron-pair donor to the electron deficient central C atom of CO_2. The polar molecules containing the second-row elements have larger BEs with CO_2 than those containing third-row elements. The dipole moments of the polar molecules significantly affect their CO_2-interactions. The increase of the atomic size or the polarizability in the same group elements has no significant effect on the electrostatic interaction component. Since the fluoric acid (HF) is a good proton donor rather than an electron donor, it shows the H-bond interaction with one electronegative O atom of CO_2 (Fig. 1).

Hydrogen cyanide (HCN) has an sp-hybrid N, which is a relatively poor electron donor and has a smaller BE with CO_2 than NH_3 does. On the other hand, for the trimethylamine (NMe$_3$)–CO_2 binding, the methyl group is electron-donating to the electro-negative N and then enhances the electrostatic interaction strength of the sp^3 N as compared with the NH_3–CO_2 binding ($-\Delta E_e = 20.3$ kJ mol^{-1} for NMe$_3$–CO_2; 14.1 kJ mol^{-1} for NH_3–CO_2). As N changes from sp^3 to sp hybridization, the CO_2-BE becomes smaller due to the contraction of the lone pair of electrons (20.3 kJ mol^{-1} for NMe$_3$–CO_2, 17.4 kJ mol^{-1} for NHCH$_2$–CO_2, 8.6 kJ mol^{-1} for HCN–CO_2). The OMe$_2$–CO_2 interaction is stronger than the H_2O–CO_2 interaction, and the OCH$_2$–CO_2 interaction has a relatively small BE among the O-containing functional systems. In CO_2–OMe$_2$/CO_2–NMe$_3$ systems, the simultaneous interactions of the electron deficient central C atom of CO_2 with the O/N atom of the functional molecules and the electron rich terminal O atoms of CO_2 with the methyl H atoms exhibit so-called cooperative intermolecular interactions, which increase the CO_2-BEs. Therefore, the sp^3-N containing functional groups (or amine-functionalization) have often been used.[26,32–34]

The fluoromethane (FCH$_3$) has a considerable CO_2-BE (10.1 kJ mol^{-1}) but this is smaller than that of fluoric acid (HF). Nevertheless, some newly designed materials with F-containing functional groups have been introduced to enhance the CO_2-adsorption enthalpy.[18,56,57] The carbonyl group (C=O) of formamide is more polar due to the resonance effect by the amino group (–NH$_2$) than that of formic acid. Thus, formamide has a stronger CO_2-BE ($-\Delta E_e = 20.7$ kJ mol^{-1}) than formic acid (20.3 kJ mol^{-1}). This explains how MOF materials functionalized by carboxylic acid work well for CO_2 capture.[58] However, no amide-functionalized material has been investigated for CO_2 capture. Amide-based materials could show considerable performance. NMe$_3$ shows strong CO_2-BE (20.3 kJ mol^{-1}). The CO_2-interaction energies of formic acid and formamide are compatible with that of NMe$_3$. Some interesting research on environmentally friendly amino acids was reported by employing the amino acids as linkers in porous solid materials for CO_2 capture in the process of CO_2 physisorption.[59] The amino acids and aminoalcohols have multiple interaction sites. Neutral amino acids and aminoalcohols can have strong intramolecular H-bonding between their hydroxyl proton and their amine N atom, which can somewhat hinder the CO_2 physisorption. 1,2,3- and 1,2,4-triazole molecules also have
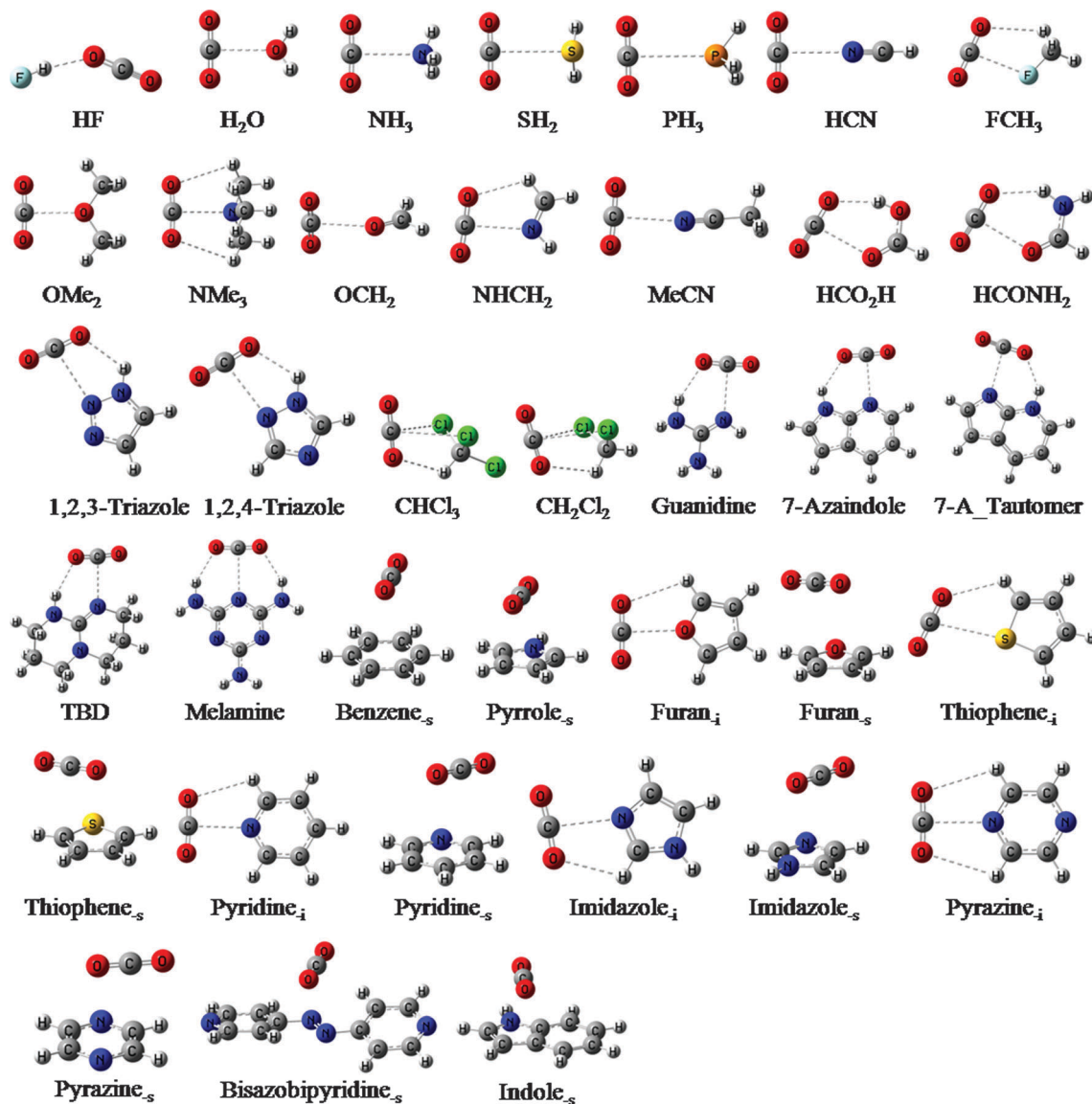
10926 | *Phys. Chem. Chem. Phys.*, 2015, **17**, 10925–10933

This journal is © the Owner Societies 2015

Fig. 1 M06-2X/aVDZ structures of various functional molecules involved in CO_2-interaction.

large CO_2-BEs (20.0 and 20.1 kJ mol^{-1}). In the CO_2–chloroform (CHCl$_3$) and CO_2–dichloromethane (CH$_2$Cl$_2$) interactions, two Cl atoms interact with the central C atom of CO_2. The CO_2 gas is somewhat soluble in both chloroform and dichloromethane solvents.[38]

3.2. Special molecules showing strong CO_2-interactions

Multi-N containing guanidine, 7-azaindole, 1,5,7-triazabicyclo-[4.4.0]dec-5-ene (TBD) and melamine are tautomerizable, showing strong amphoteric properties and having strong CO_2-bindings (24.4, 24.4, 26.9 and 27.2 kJ mol^{-1}, respectively). Guanidine and TBD are well known as superbases, and thus it is reasonable that they have large CO_2-BEs. The tautomer (7-A_Tautomer) of 7-azaindole shows a very strong CO_2-BE (29.1 kJ mol^{-1}). However, the tautomer is 13.4 kcal mol^{-1} less stable than 7-azaindole at the M06-2X/aVDZ level. Thus, this tautomer cannot be used for practical materials, and so no discussion will be made here.

Analogues and derivatives (purine BS3, imidazopyridine, adenine and imidazopyridamine) of 7-azaindole have been reported to have large CO_2 BEs.[44] At the M06-2X/aVDZ level they show large CO_2-BEs of 23.2, 24.3, 26.0 and 25.0 kJ mol^{-1}, respectively. The intriguing point is that the molecules mentioned here show larger BEs than amine species. Their stronger binding with CO_2 could imply higher selectivity than amine species. Among the molecules studied here, melamine gives the largest CO_2 BE.

3.3. π–π stacking CO_2 interactions of aromatic functional molecules

As the intermolecular interactions become important in self-assembly,[60,61] the dispersion interactions of π-systems[62–64] have recently received much attention. The CO_2-binding sometimes shows intriguing competition between electrostatic and dispersion interactions.[39–44,65–71] Aromatic systems have extra stability due to the resonance effect, which can reduce the

This journal is © the Owner Societies 2015

Phys. Chem. Chem. Phys., 2015, 17, 10925–10933 | 10927

Table 1 M06-2X/aVDZ CO_2-interaction energies (kJ mol^{-1}) with various functional molecules[a]

	$-\Delta E_e$	$-\Delta E_0$	$-\Delta H_r$
HF	12.1	7.2	9.0
H_2O	13.2	8.0	9.1
NH_3	14.1	10.6	10.5
SH_2	7.6	3.5	3.7
PH_3	5.6	2.9	1.7
HCN	8.6	7.2	6.6
FCH_3	10.1	7.4	6.5
OMe_2	17.4	15.5	14.2
NMe_3	20.3	19.6	18.2
OCH_2	9.6	6.8	5.8
$NHCH_2$	17.4	14.5	14.1
MeCN	10.5	8.6	6.9
HCO_2H	20.3	16.8	16.4
$HCONH_2$	20.7	17.4	17.1
1,2,3-Triazole	20.0	17.5	16.3
1,2,4-Triazole	20.1	17.1	16.0
$CHCl_3$	11.6	9.5	7.7
CH_2Cl_2	12.9	10.7	9.3
Guanidine	24.4	21.3	20.3
7-Azaindole	24.4	21.4	20.1
7-A_Tautomer	29.1	—	—
TBD	26.9	24.5	23.0
Melamine	27.2	22.5	22.1
Benzene$_{-s}$	10.6	9.5	7.5
Pyrrole$_{-s}$	15.7	12.6	11.4
Furan$_{-i}$	11.6	9.0	7.1
Furan$_{-s}$	10.1	7.8	6.1
Thiophene$_{-i}$	6.6	5.4	3.3
Thiophene$_{-s}$	11.3	10.9	8.7
Pyridine$_{-i}$	19.3	16.8	15.2
Pyridine$_{-s}$	11.0	8.5	6.7
Imidazole$_{-i}$	19.7	16.5	15.2
Imidazole$_{-s}$	15.1	12.3	10.9
Pyrazine$_{-i}$	17.0	14.4	12.9
Pyrazine$_{-s}$	9.0	6.6	4.8
Bisazobipyridine$_{-s}$	8.5	7.0	5.0
Indole$_{-s}$	16.7	13.1	11.5

[a] ΔE_0 is the zero-point-energy (ZPE) corrected interaction energy and ΔH_r is the enthalpy change at room temperature (298 K). Each interaction energy was corrected by the basis set superposition error (BSSE). Subscripts "-s" and "-i" indicate "stacking" and "in-plane" conformations, respectively.

degradation problem of amine cases in the regeneration cycles. Some heteroaromatic systems can have two possible interaction structures with CO_2. Subscripts "-i" and "-s" for the aromatic systems of Fig. 1 and Table 1 indicate "electrostatic in-plane" and "dispersive π–π stacking" conformations, respectively. In most cases the in-plane conformations are more stable than the stacking conformations except for the case of thiophene. The CO_2-binding of poly-thiophene was applied to CO_2 capture and CO_2 polymerization.[72,73] A poly-pyrrole shows good CO_2 adsorption capacity.[74] Pyrrole and indole do not have the in-plane conformations with CO_2. For the N-containing heteroaromatic systems (imidazole, pyridine and pyrazine), the in-plane conformations ($-\Delta E_e$ = 19.7, 19.3 and 17.0 kJ mol^{-1}) are much more stable than their stacking conformations with CO_2. For the furan, the in-plane conformation ($-\Delta E_e$ = 11.6 kJ mol^{-1}) is slightly more stable than the stacking conformation (10.1 kJ mol^{-1}) with CO_2. The stacking conformation shows somewhat weak binding strength comparable to that of benzene (10.6 kJ mol^{-1}). The attractive dispersion interaction between CO_2 and a phenyl

ring was experimentally reported.[75] The stacking conformations of N-containing pyrazine and bisazobipyridine with CO_2 give weak CO_2-BEs (9.0 and 8.5 kJ mol^{-1}). Although bisazobipyridine has small CO_2-BE, it has been applied to the functionalized MOF material to capture CO_2.[76] Heteroaromatic systems of pyrrole, thiophene, imidazole and indole show strong stacking interactions with CO_2. Among them, indole has the largest CO_2-BE (16.7 kJ mol^{-1}). Such heteroaromatic systems were reported as functional materials for CO_2 capture.[19,72–74,77–80] The stacking conformations of aromatic systems with CO_2 include the electrostatic interaction between the electronegative aromatic ring and electropositive central carbon atom of CO_2 and the bent H-bond interaction between one electropositive aromatic H atom and one electronegative O atom of CO_2, as well as the dispersion interaction.

We performed SAPT calculations at the PBE0/aVDZ level for the in-plane and stacking complexes of CO_2 with benzene, pyrrole, thiophene, pyridine and indole. Their interaction energy decompositions are analyzed in Table 2. Their electrostatic interaction energy terms (E_{es}) are over-compensated by

Table 2 DFT−SAPT interaction energy decompositions (kJ mol^{-1}) of the CO_2-interactions with functional molecules for the stacking (-s) (in-plane (-i)) conformations (E_{tot} – total interaction energy; E_{es} –electrostatic interaction energy; E_{exch}^* – exchange energy term; E_{ind}^* – induction energy term; E_{disp}^* – dispersion interaction energy)

	Benzene$_{-s}$	Pyrrole$_{-s}$	Thiophene$_{-s(-i)}$	Pyridine$_{-s(-i)}$	Indole$_{-s}$
E_{tot}	−7.98	−11.65	−8.30 (−5.68)	−6.31 (−15.74)	−12.47
E_{es}	−5.23	−10.77	−6.49 (−4.51)	−3.52 (−30.14)	−9.53
E_{exch}^*	7.12	12.40	9.12 (6.39)	5.64 (33.40)	11.53
E_{ind}^*	−0.61	−1.12	−0.74 (−0.50)	−0.46 (−3.65)	−0.99
E_{disp}^*	−8.97	−11.57	−9.80 (−6.82)	−7.77 (−13.90)	−12.95

Table 3 RI-scs-MP2/aVTZ, RI-CCSD(T)/aVTZ and RI-CCSD(T)/CBS CO_2-BEs ($-\Delta E_e$ in kJ mol^{-1}) on the RI-scs-MP2/aVTZ optimized geometries[a]

	scs-MP2	CCSD(T)/aVTZ	CCSD(T)/CBS
H_2O	10.5	11.3	11.3
NH_3	10.7	11.9	11.8
OMe_2	15.5	15.9	15.5
NMe_3	17.6	17.4	16.0
$NHCH_2$	14.4	15.1	14.9
HCO_2H	17.0	17.8	17.3
$HCONH_2$	17.5	18.5	18.1
Guanidine	20.6	21.4	23.0
7-Azaindole	23.1	23.0	(24.3)
TBD	24.1	24.3	(25.9)
Melamine	24.0	24.1	(26.4)
Benzene$_{-s}$	11.8	9.4	(10.3)
Pyrrole$_{-s}$	14.3	13.2	12.1
Furan$_{-i}$	11.5	11.7	10.8
Furan$_{-s}$	10.1	9.2	8.1
Thiophene$_{-i}$	7.3	6.8	5.2
Thiophene$_{-s}$	11.5	9.9	9.9
Pyridine$_{-i}$	17.3	17.6	16.9
Pyridine$_{-s}$	11.7	10.8	9.8
Imidazole$_{-i}$	17.5	16.4	17.3
Imidazole$_{-s}$	14.0	13.1	12.1
Indole$_{-s}$	17.5	14.6	(15.5)

[a] The values in parentheses are obtained with the CBS estimates obtained from the MP2 aVTZ and aVQZ energies and the CCSD(T) aVTZ energies.

the counter repulsive exchange interaction energy terms (E_{exch}*). In the case of benzene–CO_2 interaction, the dispersion interaction component is much larger than the electrostatic interaction component. For thiophene the stacking conformation has a large dispersion energy (-9.8 kJ mol^{-1}) in comparison with the in-plane conformation in the SAPT calculations. However, for pyridine, the electrostatic component is much larger in the in-plane conformation, and so the in-plane conformation is much more stable than the stacking conformation. The stacked thiophene–CO_2 structure has enhanced electrostatic and dispersion interaction energy components in comparison with benzene–CO_2. Pyrrole and indole have enhanced electrostatic interaction energy components and enhanced repulsive exchange interaction energy components in comparison with benzene, while they have enhanced attractive dispersion interaction energy components. Indole–CO_2 interaction has the largest dispersion interaction component among them.

All the results of the BEs of ring compounds studied here are compatible with amine species, e.g. ammonia and NMe$_3$. Moreover, unlike the amine-based wet processes, which exhibit covalent bond breaking, followed by amine loss, the aromatic ring compounds are not expected to have such chemical reactions due to their non-covalent stacking interactions, and thus show no significant amine loss. Therefore, they can be applied to develop novel materials to capture the CO_2 gas.

3.4. High level calculations of strong CO_2-interaction systems

Based on the M06-2X BEs of the functional molecules with a CO_2 molecule, we selected important complexes and calculated their optimal structures and interaction energies at the RI-scs-MP2/aVTZ level. The RI-CCSD(T)/CBS BEs were estimated by the RI-CCSD(T)/aVTZ and RI-CCSD(T)/aVQZ single point calculations at the RI-scs-MP2/aVTZ geometries. These CO_2-BEs ($-\Delta E_e$) are given in Table 3. Their RI-scs-MP2/aVTZ structures are shown in Fig. 2. Based on the RI-CCSD(T)/CBS BEs, NMe$_3$ has a large CO_2-BE (16.0 kJ mol^{-1}). The CO_2-BEs of formamide and formic acid are 18.1 and 17.3 kJ mol^{-1}, respectively, which are larger than that of NMe$_3$. The tautomerizable multi-N-containing systems (guanidine, 7-azaindole, TBD and melamine) show much larger CO_2-BEs (23.0, 24.3, 25.9, and 26.4 kJ mol^{-1}, respectively). Amine, carboxylic acid and amide
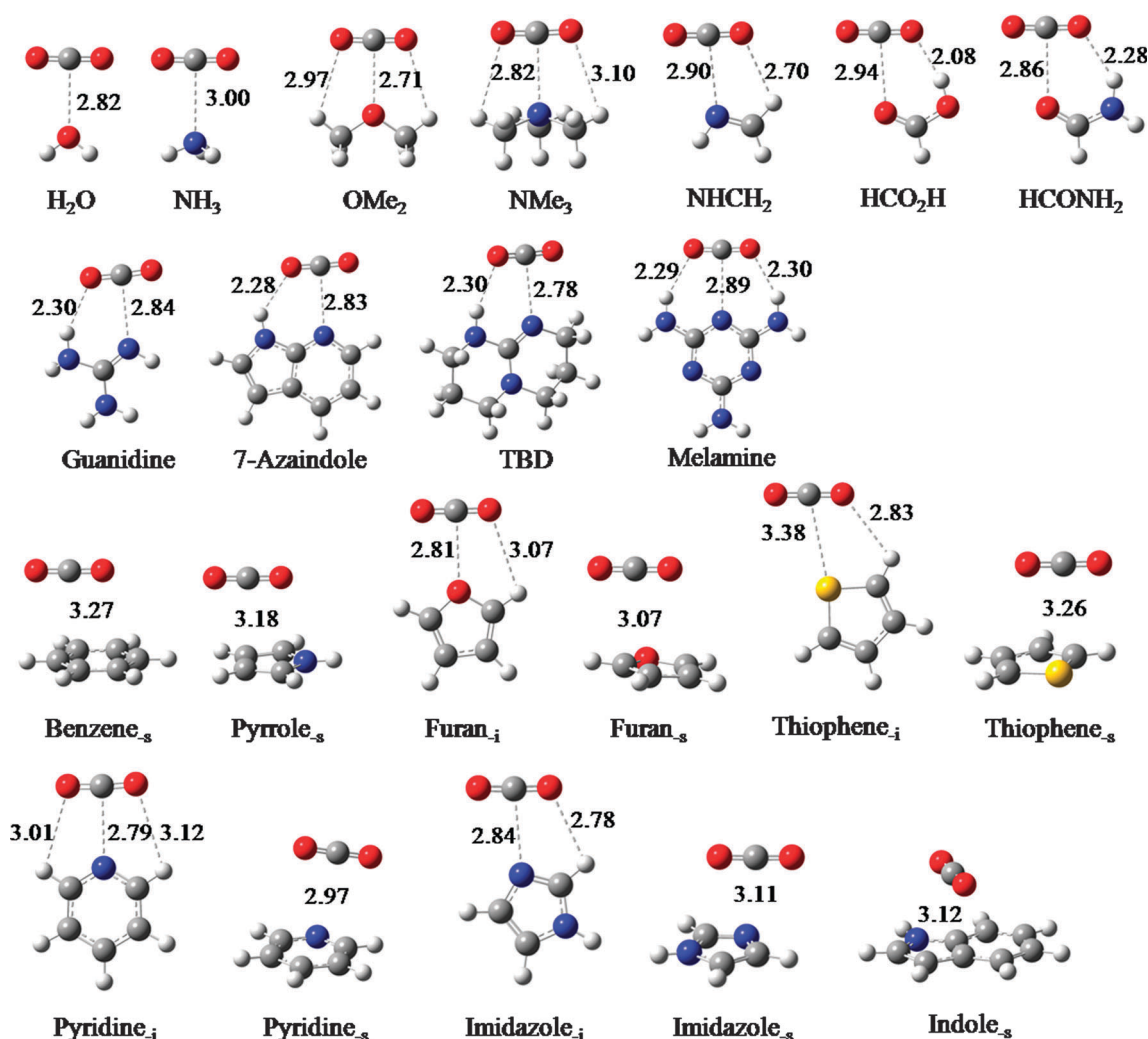

Fig. 2 RI-scs-MP2/aVTZ structures of selected functional molecules involved in the CO_2-interaction.

have considerably large CO_2-BEs. Pyridine and imidazole have larger CO_2-BEs (16.9 and 17.3 kJ mol^{-1}) than NMe$_3$ due to larger dipole moments (2.24/2.33 Debye for pyridine, 3.86/3.85 Debye for imidazole, and 0.62/0.79 Debye for NMe$_3$ at the M06-2X/RI-CCSD(T) level). This effect also appears in the 7-azaindole–CO_2 interaction. The CO_2-BE of indole is 15.5 kJ mol^{-1}. A polymer synthesized with indole shows a larger CO_2 adsorption enthalpy (49.0 kJ mol^{-1}) at zero coverage, which is much more than three times the CO_2–indole BE due to the cooperative interactions.[19] This indicates the binding of a CO_2 molecule mostly with three indole molecules and sometimes with four indole molecules. The BE of a CO_2 molecule with one indole molecule is 15.5 kJ mol^{-1}, and so the CO_2-BEs with three and four indole molecules can be roughly estimated to be 41.5 and 62 kJ mol^{-1}, respectively, when the binding is assumed not to be seriously disturbed by the presence other indole molecules. This could be possible because the CO_2–indole interaction is based on the stacking interaction, and the three or four fold interactions with one CO_2 molecule the same could be feasible when the stackings are made in the shape of three or four propeller blades of indole surrounding the linear CO_2 molecular axis (see, for example, Fig. 3). In reality, the side H-bond interaction of the CO_2–indole system would be no more than that

of the CO_2–water system in which the OC=O$\cdots$H–OH interaction energy was 5.5 kJ mol^{-1}.[40] Indole is an extended derivative of pyrrole, and carbazole is a larger extended derivative of indole. Among them, indole shows the strongest stacking interaction with CO_2.[19] The bigger aromatic systems do not show larger CO_2-BEs.

3.5. Applications of functional molecules to CO_2 capture

In CO_2 capture, not only does CO_2-BE affect the selectivity but also the molecular weight of the absorbent affecting the weight capacity is an important factor. NMe$_3$, formic acid, formamide, guanidine, 7-azaindole, TBD, and melamine show large CO_2-BEs and their molecular weights are 59, 46, 45, 59, 118, 139, and 126 g mol^{-1}, respectively. However, melamine has three CO_2-binding sites and then the weight of melamine per CO_2 is 42 g mol^{-1}, which shows an extremely impressive weight capacity. Formic acid and formamide have small molecular weights and large CO_2-BEs. Formamide has a larger CO_2-BE than formic acid. The CO_2 interacting systems of amides were experimentally studied in the vapor–liquid equilibrium state.[81] However, formamide is a liquid in the standard state. Since the amide–amide interaction is very strong ($-\Delta E_e = 60.2$ kJ mol^{-1} at the M06-2X level), CO_2 cannot be dissolved in the formamide solvent.

Imidazole-4-amide 22.4

Imidazole-2-imine 23.6

CO_2-4 7-Azaindole 53.8

CO_2-2Melamine 47.9

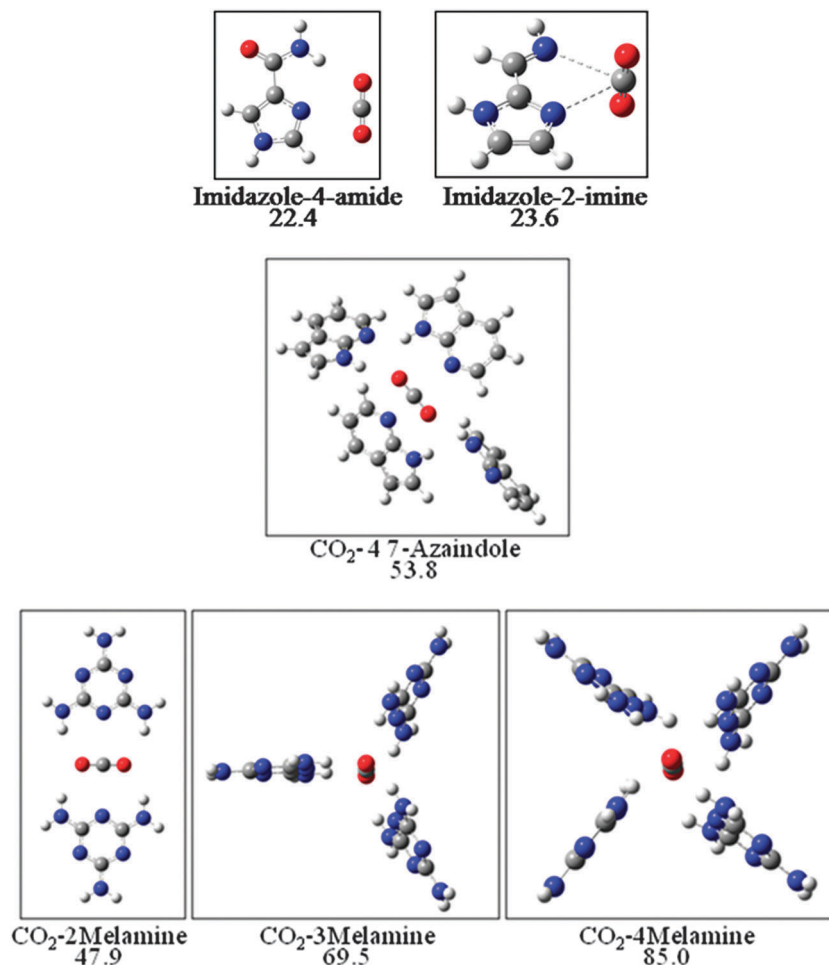**CO_2-3Melamine** 69.5

CO_2-4Melamine 85.0

Fig. 3 Designed systems for CO_2 capture. The values are BEs ($-\Delta E_e$) in kJ mol^{-1} at the M06-2X/aVDZ level.

As exemplary host systems using imidazole, formamide and imine, we can designed imidazole-4-amide and imidazole-2-imine, as shown in Fig. 3. The CO_2-BEs of imidazole-4-amide and imidazole-2-imine ($-\Delta E_e$ = 22.4 and 23.6 kJ mol^{-1}, respectively), are larger than those of imidazole, formamide and imine (19.7, 20.7, and 18.2 kJ mol^{-1}) and that of imidazole-2-carboxylic acid (21.5 kJ mol^{-1}). Thus, the imidazole-4-amide and imidazole-2-imine molecules show impressive CO_2 BEs. Indeed, an analogue of imidazole-4-amide was already synthesized and reported as a polymer.[82] Dacarbazine as a derivative of imidazole-4-amide is a well-known chemical. The imidazole-2-imine moiety is also found in many imidazole derivatives.

Indole was also successfully used in the polymer form to capture CO_2 gas.[19] In our study, guanidine, 7-azaindole, TBD and melamine show large CO_2-BEs. Among them, 7-azaindole has a similar structure to indole. It is not easy to synthesize the 7-azaindole functional group into polymers due to the difficult oxidation reaction of 7-azaindole. However, if 7-azaindole is used as a functional unit of the materials for CO_2 capture, such materials could show high selectivity for CO_2 capture due to the large CO_2-BE of 7-azaindole ($-\Delta E_e$ = 24.4 kJ mol^{-1} at the M06-2X/aVDZ level). The CO_2-BE of indole is 17.5 kJ mol^{-1} at the M06-2X level. As mentioned in the previous section, CO_2 can interact with up to four 7-azaindole molecules (Fig. 3), as the experiment showed the CO_2 adsorption enthalpy of -49 kJ mol^{-1} at zero coverage of indole,[19] which indicates the interactions with 3 to 4 indole molecules. In this tetra-coordination, the CO_2-BE is calculated to be 53.8 kJ mol^{-1} ($-\Delta E_e$) at the M06-2X/aVDZ level. The large adsorption enthalpy is critical to the high capacity and selectivity for CO_2 in the gas mixture.

A guanidine-functional polymer was reported to show good performance at high temperature.[83] Several applications of melamine were reported to show high capacity for CO_2 capture.[84,85] However, in most cases the central triazine ring was used as one or two stacking CO_2-binding sites which have three N atoms,[86] which resulted in relatively weak CO_2-BE. Melamine-terminal materials could show better performance due to the effective electrostatic CO_2-binding as shown in Fig. 1 and 2. As shown in a model system (Fig. 3), CO_2-two melamines, CO_2-three melamines and CO_2-four melamines show large CO_2-BEs (47.9, 69.5 and 85.0 kJ mol^{-1}, respectively) at the M06-2X/aVDZ level. Such large values arise from the maximized electrostatic interactions between CO_2 and melamine molecules associated with four-fold triple bindings comprised of two $O^{\delta-}\cdots H^+ N^{\delta-}$ electrostatic H-bonds and one $C^{\delta+}\cdots N^{\delta-}$ electrostatic bond. These model systems show much higher CO_2-BEs. The multi-N-containing molecules (guanidine, 7-azaindole, TBD, and melamine) with large CO_2-BEs could be used as multi-binding sites for a CO_2 molecule in devising absorbent materials with large CO_2 adsorption enthalpies.

4. Concluding remarks

Tautomerizable multi-N-containing strong bases (guanidine, 7-azaindole, TBD, and melamine) show considerably strong electrostatic interactions with CO_2 due to their strong amphoteric properties. Among them, melamine shows the largest CO_2-electrostatic BE. The stronger binding between these functional molecules with CO_2 could imply better selectivity than the amine species. Among the various aromatic systems considered, indole shows the largest dispersion interaction energy with CO_2. The chemical units with large CO_2-BEs could be applied to devising functional materials for efficient CO_2 capture. Furthermore, CO_2 by tetra coordination of melamines gives a very large CO_2-BE (85.0 kJ mol^{-1}). Thus, multi-N-containing molecules (guanidine, 7-azaindole, TBD, and melamine) with large CO_2-BEs could be used as multi-binding sites for a CO_2 molecule. The present results could provide useful information for the development of promising functionalized materials for CO_2 capture/sequestration.

References

1 A. A. Lacis, G. A. Schmidt, D. Rind and R. A. Ruedy, *Science*, 2010, **330**, 356–359.
2 J. D. Shakun, P. U. Clark, F. He, S. A. Marcott, A. C. Mix, Z. Liu, B. Otto-Bliesner, A. Schmittner and E. Bard, *Nature*, 2012, **484**, 49–54.
3 M. Garner, A. Attwood, D. S. Baldwin, A. James and M. R. Munafo, *Neuropsychopharmacology*, 2011, **36**, 1557–1562.
4 D. M. D'Alessandro, B. Smit and J. R. Long, *Angew. Chem., Int. Ed.*, 2010, **49**, 6058–6082.
5 C. Lastoskie, *Science*, 2010, **330**, 595–596.
6 H. Li, P. H. Opgenorth, D. G. Wernick, S. Rogers, T.-Y. Wu, W. Higashide, P. Malati, Y.-X. Huo, K. M. Cho and J. C. Liao, *Science*, 2012, **335**, 1596.
7 P. Markewitz, W. Kuckshinrichs, W. Leiter, J. Linssen, P. Zapp, R. Bongartz, A. Schreiber and T. E. Muller, *Energy Environ. Sci.*, 2012, **5**, 7281–7305.
8 C.-H. Huang and C.-S. Tan, *Aerosol Air Qual. Res.*, 2014, **14**, 480–499.
9 P. Nugent, Y. Belmabkhout, S. D. Burd, A. J. Cairns, R. Luebke, K. Forrest, T. Pham, S. Ma, B. Space, L. Wojtas, M. Eddaoudi and M. J. Zaworotko, *Nature*, 2013, **495**, 80–84.
10 D.-X. Xue, A. J. Cairns, Y. Belmabkhout, L. Wojtas, Y. Liu, M. H. Alkordi and M. Eddaoudi, *J. Am. Chem. Soc.*, 2013, **135**, 7660–7667.
11 R. Poloni, B. Smit and J. B. Neaton, *J. Am. Chem. Soc.*, 2012, **134**, 6714–6719.
12 L. Du, Z. Lu, K. Zheng, J. Wang, X. Zheng, Y. Pan, X. You and J. Bai, *J. Am. Chem. Soc.*, 2013, **135**, 562–565.

This journal is © the Owner Societies 2015

Phys. Chem. Chem. Phys., 2015, **17**, 10925–10933 | 10931

13 H. Amrouche, S. Aguado, J. Perez-Pellitero, C. Chizallet, F. Siperstein, D. Farrusseng, N. Bats and C. Nieto-Draghi, *J. Phys. Chem. C*, 2011, **115**, 16425–16432.

14 J. A. Thompson, N. A. Brunelli, R. P. Lively, J. R. Johnson, C. W. Jones and S. Nair, *J. Phys. Chem. C*, 2013, **117**, 8198–8207.

15 R. Babarao, R. Custelcean, B. P. Hay and D. Jiang, *Cryst. Growth Des.*, 2012, **12**, 5349–5356.

16 F. Rezaei, R. P. Lively, Y. Labreche, G. Chen, Y. Fan, W. J. Koros and C. W. Jones, *ACS Appl. Mater. Interfaces*, 2013, **5**, 3921–3931.

17 Y. Kuwahara, D.-Y. Kang, J. R. Copeland, N. A. Brunelli, S. A. Didas, P. Bollini, C. Sievers, T. Kamegawa, H. Yamashita and C. W. Jones, *J. Am. Chem. Soc.*, 2012, **134**, 10757–10760.

18 E. Girard, T. Tassaing, S. Camy, J.-S. Condoret, J.-D. Marty and M. Destarac, *J. Am. Chem. Soc.*, 2012, **134**, 11920–11923.

19 M. Saleh, H. M. Lee, K. C. Kemp and K. S. Kim, *ACS Appl. Mater. Interfaces*, 2014, **6**, 7325–7333.

20 H. Choi, Y. C. Park, Y.-H. Kim and Y. S. Lee, *J. Am. Chem. Soc.*, 2011, **133**, 2084–2087.

21 F. A. Chowdhury, H. Yamada, T. Higashii, K. Goto and M. Onoda, *Ind. Eng. Chem. Res.*, 2013, **52**, 8323–8331.

22 Y. Matsuzaki, H. Yamada, F. A. Chowdhury, T. Higashii and M. Onoda, *J. Phys. Chem. A*, 2013, **117**, 9274–9281.

23 B. Han, C. Zhou, J. Wu, D. J. Tempel and H. Cheng, *J. Phys. Chem. Lett.*, 2011, **2**, 522–526.

24 D. Y. Kim, H. M. Lee, S. K. Min, Y. Cho, I-C. Hwang, K. Han, J. Y. Kim and K. S. Kim, *J. Phys. Chem. Lett.*, 2011, **2**, 689–694.

25 X. Luo, Y. Guo, F. Ding, H. Zhao, G. Cui, H. Li and C. Wang, *Angew. Chem., Int. Ed.*, 2014, **53**, 7053–7057.

26 I. Niedermaier, M. Bahlmann, C. Papp, C. Kolbeck, W. Wei, S. K. Calderon, M. Grabau, P. S. Schulz, P. Wasserscheid, H.-P. Steinruck and F. Maier, *J. Am. Chem. Soc.*, 2014, **136**, 436–441.

27 E. F. da Silva, H. Lepaumier, A. Grimstvedt, S. J. Vevelstad, A. Einbu, K. Vernstad, H. F. Svendsen and K. Zahlsen, *Ind. Eng. Chem. Res.*, 2012, **51**, 13329–13338.

28 C. S. Srikanth and S. S. C. Chuang, *J. Phys. Chem. C*, 2013, **117**, 9196–9205.

29 X. Ge, S. L. Shaw and Q. Zhang, *Environ. Sci. Technol.*, 2014, **48**, 5066–5075.

30 Y. S. Yu, H. F. Lu, T. T. Zhang, Z. X. Zhang, G. X. Wang and V. Rudolph, *Ind. Eng. Chem. Res.*, 2013, **52**, 12622–12634.

31 N. Gargiulo, F. Pepe and D. Caputo, *J. Nanosci. Nanotechnol.*, 2014, **14**, 1811–1822.

32 S. Choi, T. Watanabe, T.-H. Bae, D. S. Sholl and C. W. Jones, *J. Phys. Chem. Lett.*, 2012, **3**, 1136–1141.

33 R. Vaidhyanathan, S. S. Iremonger, G. K. H. Shimizu, P. G. Boyd, S. Alavi and T. K. Woo, *Angew. Chem., Int. Ed.*, 2012, **51**, 1826–1829.

34 R. Haldar, S. K. Reddy, V. M. Suresh, S. Mohapatra, S. Balasubramanian and T. K. Maji, *Chem. – Eur. J.*, 2014, **20**, 4347–4356.

35 S. Wang, W.-C. Li, L. Zhang, Z.-Y. Jin and A.-H. Lu, *J. Mater. Chem. A*, 2014, **2**, 4406–4412.

36 S. Biswas, D. E. P. Vanpoucke, T. Verstraelen, M. Vandichel, S. Couck, K. Leus, Y.-Y. Liu, M. Waroquier, V. V. Speybroeck, J. F. M. Denayer and P. V. D. Voort, *J. Phys. Chem. C*, 2013, **117**, 22784–22796.

37 E. N. Lay, V. Taghikhani and C. Ghotbi, *J. Chem. Eng. Data*, 2006, **51**, 2197–2200.

38 K. Shirono, T. Morimatsu and F. Takemura, *J. Chem. Eng. Data*, 2008, **53**, 1867–1871.

39 K. M. de Lange and J. R. Lane, *J. Chem. Phys.*, 2011, **135**, 064304.

40 J. Makarewicz, *J. Chem. Phys.*, 2010, **132**, 234305.

41 A. Torrisi, C. Mellot-Draznieks and R. G. Bell, *J. Chem. Phys.*, 2009, **130**, 194703.

42 A. Torrisi, C. Mellot-Draznieks and R. G. Bell, *J. Chem. Phys.*, 2010, **132**, 044705.

43 L. Chen, F. Cao and H. Sun, *Int. J. Quantum Chem.*, 2013, **113**, 2261–2266.

44 K. D. Vogiatzis, A. Mavrandonakis, W. Klopper and G. E. Froudakis, *ChemPhysChem*, 2009, **10**, 374–383.

45 Y. Zhao and D. G. Truhlar, *J. Phys. Chem. A*, 2006, **110**, 5121–5129.

46 M. Gerenkamp and S. Grimme, *Chem. Phys. Lett.*, 2004, **392**, 229–235.

47 S. Grimme, *J. Chem. Phys.*, 2003, **118**, 9095–9102.

48 M. Kolaski, A. Kumar, N. J. Singh and K. S. Kim, *Phys. Chem. Chem. Phys.*, 2011, **13**, 991–1001.

49 T. Helgaker, W. Klopper, H. Koch and J. Noga, *J. Chem. Phys.*, 1997, **106**, 9639–9646.

50 S. K. Min, E. C. Lee, H. M. Lee, D. Y. Kim, D. Kim and K. S. Kim, *J. Comput. Chem.*, 2008, **29**, 1208–1221.

51 R. Vaidhyanathan, S. S. Iremonger, G. K. H. Shimizu, P. G. Boyd, S. Alavi and T. K. Woo, *Science*, 2010, **330**, 650–653.

52 A. Heßelmann, G. Jansen and M. Schütz, *J. Chem. Phys.*, 2005, **122**, 014103.

53 E. C. Lee, D. Kim, P. Jurečka, P. Tarakeshwar, P. Hobza and K. S. Kim, *J. Phys. Chem. A*, 2007, **111**, 3446–3457.

54 TURBOMOLE V6.4 2012; a development of University of Karlsruhe and Forschungszentrum Karlsruhe GmbH, Karlsruhe, Germany, 2007, available from http://www.turbomole.com.

55 H.-J. Werner, P. J. Knowles, R. Lindh, F. R. Manby, M. Schutz, P. Celani, T. Korona, G. Rauhut, R. D. Amos, A. Bernhardsson, A. Berning, D. L. Cooper, M. J. O. Deegan, A. J. Dobbyn, F. Eckert, C. Hampel, G. Hetzer, A. W. Lloyd, S. J. McNicholas, W. Meyer, M. E. Mura, A. Nicklass, P. Palmieri, R. Pitzer, U. Schumann, H. Stoll, A. J. Stone, R. Tarroni and T. Thorsteinsson, *MOLPRO, a package of ab initio programs, version 2006.1*, Institut für Theoretische Chemie, Universität Stuttgart, Stuttgart, Germany, 2006.

56 D.-S. Zhang, Z. Chang, Y.-F. Li, Z.-Y. Jiang, Z.-H. Xuan, Y.-H. Zhang, J.-R. Li, Q. Chen, T.-L. Hu and X.-H. Bu, *Sci. Rep.*, 2013, **3**, 3312.

57 J. J. Nogueira, S. A. Vazquez, U. Lourderaj, W. L. Hase and E. Martinez-Nunez, *J. Phys. Chem. C*, 2010, **114**, 18455–18464.

58 Z. Xiang, S. Leng and D. Cao, *J. Phys. Chem. C*, 2012, **116**, 10573–10579.

10932 | *Phys. Chem. Chem. Phys.*, 2015, **17**, 10925–10933

This journal is © the Owner Societies 2015

59 M. A. Hussain, Y. Soujanya and G. N. Sastry, *Environ. Sci. Technol.*, 2011, **45**, 8582–8588.

60 J. Y. Lee, B. H. Hong, D. Y. Kim, D. R. Mason, J. W. Lee, Y. Chun and K. S. Kim, *Chem. – Eur. J.*, 2013, **19**, 9118–9122.

61 J. Y. Lee, B. H. Hong, W. Y. Kim, S. K. Min, Y. Kim, M. V. Jouravlev, R. Bose, K. S. Kim, I.-C. Hwang, L. J. Kaufman, C. W. Wong, P. Kim and K. S. Kim, *Nature*, 2009, **460**, 498–501.

62 Y. Cho, W. J. Cho, I. S. Youn, G. Lee, N. J. Singh and K. S. Kim, *Acc. Chem. Res.*, 2014, **47**, 3321–3330.

63 S. K. Min, W. Y. Kim, Y. Cho and K. S. Kim, *Nat. Nanotechnol.*, 2011, **6**, 162–165.

64 N. J. Singh, S. K. Min, D. Y. Kim and K. S. Kim, *J. Chem. Theory Comput.*, 2009, **5**, 515–529.

65 Y. F. Chen, J. Y. Lee, R. Babarao, J. Li and J. W. Jiang, *J. Phys. Chem. C*, 2010, **114**, 6602–6609.

66 S. S. Han, D. Kim, D. H. Jung, S. Cho, S.-H. Choi and Y. Jung, *J. Phys. Chem. C*, 2012, **116**, 20254–20261.

67 C. M. Tenney and C. M. Lastoskie, *Environ. Prog.*, 2006, **25**, 343–354.

68 S. Vaupel, B. Brutschy, P. Tarakeshwar and K. S. Kim, *J. Am. Chem. Soc.*, 2006, **128**, 5416–5426.

69 E. C. Lee, B. H. Hong, J. Y. Lee, J. C. Kim, D. Kim, Y. Kim, P. Tarakeshwar and K. S. Kim, *J. Am. Chem. Soc.*, 2005, **127**, 4530–4537.

70 K. Muller-Dethlefs and P. Hobza, *Chem. Rev.*, 2000, **100**, 143–167.

71 J.-H. Choi and J.-H. Cho, *J. Am. Chem. Soc.*, 2006, **128**, 3890–3891.

72 C.-C. Hwang, J. J. Tour, C. Kittrell, L. Espinal, L. B. Alemany and J. M. Tour, *Nat. Commun.*, 2014, **5**, 3961.

73 S. L. Qiao, Z. K. Du, W. Huang and R. Q. Yang, *J. Solid State Chem.*, 2014, **212**, 69–72.

74 V. Chandra, S. U. Yu, S. H. Kim, Y. S. Yoon, D. Y. Kim, A. H. Kwon, M. Meyyappan and K. S. Kim, *Chem. Commun.*, 2012, **48**, 735–737.

75 D. Kajiya and K. Saitow, *J. Phys. Chem. B*, 2010, **114**, 16832–16837.

76 R. Dey, R. Haldar, T. K. Maji and D. Ghoshal, *Cryst. Growth Des.*, 2011, **11**, 3905–3911.

77 M. G. Rabbani and H. M. El-Kaderi, *Chem. Mater.*, 2011, **23**, 1650–1653.

78 M. S. Shannon, J. M. Tedstone, S. P. O. Danielsen, M. S. Hindman and J. E. Bara, *Energy Fuels*, 2013, **27**, 3349–3357.

79 M. Prakash, K. Mathivon, D. M. Benoit, G. Chambaud and M. Hochlaf, *Phys. Chem. Chem. Phys.*, 2014, **16**, 12503–12509.

80 S. Altarawneh, S. Behera, P. Jena and H. M. El-Kaderi, *Chem. Commun.*, 2014, **50**, 3571–3574.

81 H.-S. Byun, N.-H. Kim and C. Kwak, *Fluid Phase Equilib.*, 2003, **208**, 53–68.

82 S.-Y. Duan, X.-M. Ge, N. Lu, F. Wu, W. Yuan and T. Jin, *Int. J. Nanomed.*, 2012, **7**, 3813–3822.

83 M. A. Alkhabbaz, R. Khunsupat and C. W. Jones, *Fuel*, 2014, **121**, 79–85.

84 K. Ahmad, O. Nowla, E. M. Kennedy, B. Z. Dlugogorski, J. C. Mackie and M. Stockenhuber, *Energy Technol.*, 2013, **1**, 345–349.

85 J.-X. Hu, H. Shang, J.-G. Wang, L. Luo, Q. Xiao, Y.-J. Zhong and W.-D. Zhu, *Ind. Eng. Chem. Res.*, 2014, **53**, 11828–11837.

86 M. Saleh, S. B. Baek, H. M. Lee and K. S. Kim, *J. Phys. Chem. C*, 2015, **119**, 5395–5402.

This journal is © the Owner Societies 2015

Phys. Chem. Chem. Phys., 2015, **17**, 10925–10933 | 10933